Optimized V-shape design of GaN nanodiodes for the generation of Gunn oscillations

J.-F. Millithaler,[1] I. Iñiguez-de-la-Torre,[1] A. Iñiguez-de-la-Torre,[1] T. González,[1] P. Sangaré,[2] G. Ducournau,[2] C. Gaquière,[2] and J. Mateos[1,a)]
[1]*Departamento de Física Aplicada, Universidad de Salamanca, Plaza de la Merced s/n, 37008 Salamanca, Spain*
[2]*Institut d'Electronique de Microélectronique et de Nanotechnologie (IEMN), UMR CNRS 8520, Université de Lille 1, Avenue Poincaré BP60069, 59652, Villeneuve d'Ascq CEDEX, France*

(Received 19 November 2013; accepted 4 February 2014; published online 20 February 2014)

In this work, recent advances in the design of GaN planar Gunn diodes with asymmetric shape, so-called self-switching diodes, are presented. A particular geometry for the nanodiode is proposed, referred as V-shape, where the width of the channel is intentionally increased as approaching the anode. This design, which reduces the effect of the surface-charges at the anode side, is the most favourable one for the onset of Gunn oscillations, which emerge at lower current levels and with lower threshold voltages as compared to the standard square geometry, thus enhancing the power efficiency of the self-switching diode as sub-millimeter wave emitters. © *2014 AIP Publishing LLC*. [http://dx.doi.org/10.1063/1.4866166]

One big challenge for both the fields of electronics and optics is to conquer the least explored region of the electromagnetic spectrum, the so-called "terahertz (THz) gap." Situated between the far infrared and the millimeter wave ranges, it offers a wide range of interesting applications like ultra-high speed telecommunications, medical diagnosis, and astronomy of security control.[1,2] However, commercial applications in the THz range are difficult to implement due to the lack of cheap and compact sources and detectors. Many efforts are being made to overcome the performances of Schottky barrier diode-based detectors and laser-based THz generators.

One promising way to build up both emitters and detectors on the same chip is the use of the self-switching diode (SSD), originally proposed by Song.[3] A rectifying I-V characteristic can be easily obtained with a remarkably simple fabrication process, by just etching two L-shaped insulating trenches onto a semiconductor layer. Taking advantage of such non-linearity, SSDs fabricated with different technologies have already shown experimentally extraordinary capabilities for THz detection, both in a guided setup and in free space. GaAs SSDs have demonstrated room temperature detection at 1.5 THz,[4] and even up to 2.5 THz at 10 K.[5] Recently, successful results have been obtained also with InAs SSDs at 600 GHz.[6] The use of such narrow bandgap semiconductors will allow to largely overcome the frequency performances of GaAs SSDs. On the other hand, SSDs made on GaN, in spite of the lower mobility of such wide bandgap semiconductor, have also shown detection functionality up to 320 GHz.[7] In this material, the strategic combination of such an ingenious geometry with the presence of negative differential mobility, high electrical strength, high saturation velocity, and low energy relaxation time, offers an optimal environment for the generation of very high frequency Gunn oscillations.[8,9] Moreover, the planar geometry of the SSDs allows not only the easy integration of antennas for a better free space coupling and a flexibility in the design (for an optimum thermal dissipation and reduction of parasitic effects) but also opens the possibility to develop a completely integrated room-temperature emitter/detector THz system working at room temperature.

Previous works of our team, performed by means of Monte Carlo (MC) simulations, have already explained the physics of the DC and AC operation of SSDs as well as their noise properties.[10,11] Regarding to their operation as Gunn diodes, it has also been shown that the nucleation and fast transit of high-field domains is promoted by the shape of the SSD.[9] Prior works of our group[12] have demonstrated the technological feasibility of GaN SSDs and foresee the possibility to generate power in the sub-THz frequency band. Even if this prediction has not been experimentally demonstrated yet, in this paper we report on an improvement of the original design by leaning the trenches to obtain a V-shape channel that enhances the Gunn signal with a decrease of the operating DC current and voltage which alleviate thermal limitations and reliability aspects.

Concerning the modeling of the devices, we use a semi-classical MC simulator self-consistently coupled with a two-dimensional (2D) Poisson solver.[13] To account for the three dimensional (3D) nature of the diodes, a background doping N_{Db} (here $5 \times 10^{17}\,cm^{-3}$) is considered when solving Poisson equation, and a surface charge density σ is placed at the semiconductor-dielectric boundaries of the insulating trenches. The value of σ is self-consistently updated with the electron concentration in the nearby region in order to reproduce the correct behavior of the device.[14] Details about the model can be found in Refs. 12, 15, and 16. For the frequency analysis of the current sequences we make use of the fast Fourier transform (FFT). The dynamics of electrons in the device is simulated during time series of 500.000 steps of 1 fs for each bias point.

Fig. 1 schematically shows the geometry of the simulated devices. They are based on an AlGaN/GaN heterostructure

a)Author to whom correspondence should be addressed. Electronic mail: javierm@usal.es

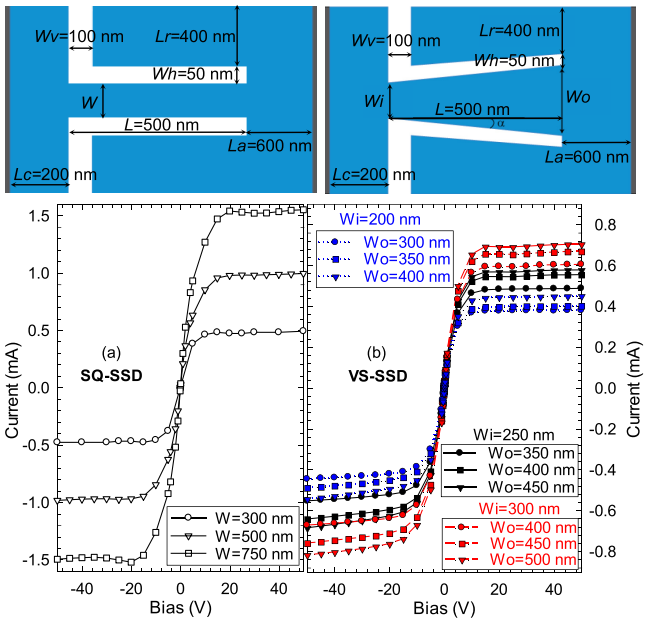

FIG. 1. I-V curves at 300 K for (a) SQ-SSDs and (b) VS-SSDs (with the geometries sketched at the top), for a length $L = 500$ nm and different widths of the channel.

with a sheet carrier density of 5×10^{12} cm^{-2}. Two L-shape trenches define the asymmetric nano-channel. We can distinguish two types of SSDs: (i) the regular (square) one denoted as SQ-SSD, where the long trenches are horizontal, providing a constant channel width (W); (ii) the "V-shape" one, called VS-SSD, with leaned trenches, resulting in a channel with a smaller width at the entrance, W_i, than at the exit, W_o. The length of the channel in all simulated devices is $L = 500$ nm, so that the general criteria for the onset of Gunn oscillations in bulk GaN $n \times L \geq 8 \times 10^{12}$ cm^{-2} (with n the electron concentration) is fulfilled.[7,17]

The horizontal and vertical widths of the trenches, $W_v = 100$ nm and $W_h = 50$ nm, respectively, are well in the range of the technologically achievable dimensions.[12] The length of the cathode (L_c) and anode (L_a) access regions, as well as the lateral dimension (L_r), have been chosen in the simulations as the smallest possible ones in order to reduce the calculation time, but large enough to allow the correct modeling of the device. Their values are $L_c = 200$ nm, $L_a = 600$ nm, and $L_r = 400$ nm. All simulations are carried out at room temperature with the left terminal grounded.

Originally, SSDs were designed with narrow channels to behave as rectifying diodes,[3] switched off when a negative voltage is applied to the right terminal, with the channel depleted due to the lateral electric field and the negative charges at the walls of the trenches, and switched on when a positive voltage allows the opening of the channel.[3,10] When the width of the channel of the SSD is enlarged, its I-V characteristic becomes almost symmetric, as observed in Fig. 1, but its special geometry provides an adequate playground for the generation of Gunn oscillations. The current of the SQ-SSDs are much higher due to their larger width, but with the same width at the entrance the current level is increased with the use of the V-shaped channel. If we compare, the case of the SQ-SSD with $W = 300$ nm, Fig. 1(a), provides a maximum current of about 0.5 mA while, for the VS-SSD with the same W_i, Fig. 1(b), the current level can be increased up to 0.7 mA.

In a first attempt to compare the performances of SQ-SSDs and VS-SSDs, Fig. 2 shows the current sequences of both types of structures for increasing bias in the range 0 to 30 V. The width of the SQ-SSDs ranges from 300 to 750 nm while W_i is varying from 200 to 300 nm in the case of the VS-SSDs (the leaning angle is kept constant to about 6°, by using $W_o = W_i + 100$ nm). The good agreement with the values of DC current measured in real devices confirms the validity of the MC model used.

It can be observed in Fig. 2 that even if the primary condition about $n \times L$ is fulfilled by using $L = 500$ nm, a sufficiently wide channel, of about 500 nm, is required to generate Gunn oscillations in SQ-SSDs, with a threshold voltage of about 25 V. For the VS-SSDs, a much narrower entrance width of 300 nm is enough for allowing the onset of the oscillations (thus at a smaller current level), with the additional advantage that the threshold voltage is decreased to 20 V. In addition, the ratio between the amplitude of the AC and DC currents increases from a 10% in the SQ-SSD up to 17.5% in the VS-SSD. The values of the oscillation frequency, f_{Gunn}, are similar in all the cases, around 400 GHz, since it is mainly determined by the length of the channel.

It is therefore clear that the leaning of the trenches benefits the onset of Gunn oscillations and reduces the level of input DC power needed (which is approximately halved, from about 25 mW per SQ-SSD down to 12 mW per VS-SSD), thus strongly lowering heat dissipation, which is one of the key issues for achieving a practical demonstration

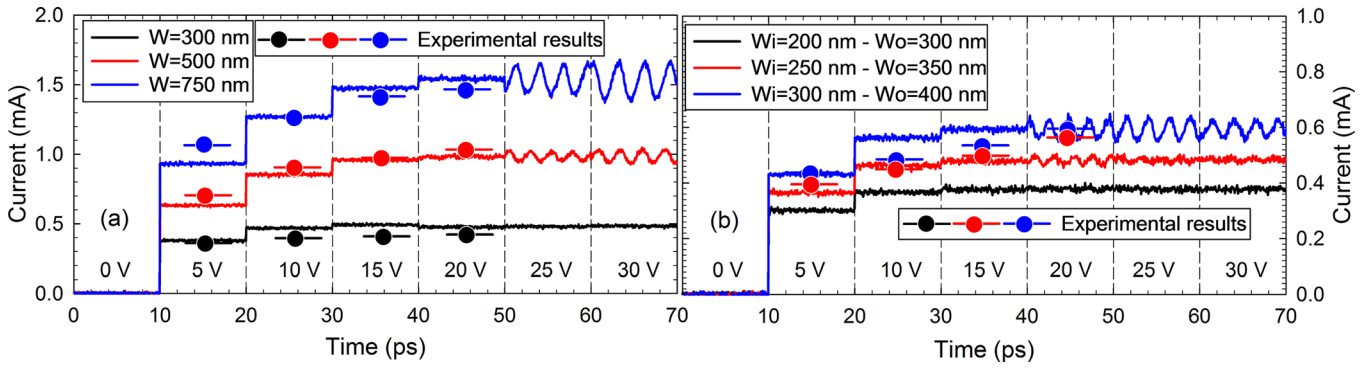

FIG. 2. Simulated time sequences of the current for a bias range from 0 to 30 V, at room temperature, for (a) SQ-SSDs and (b) VS-SSDs, for a length $L = 500$ nm and different widths of the channel. For comparison, the experimental DC current measured in real devices with the same geometries is also plotted (circles).

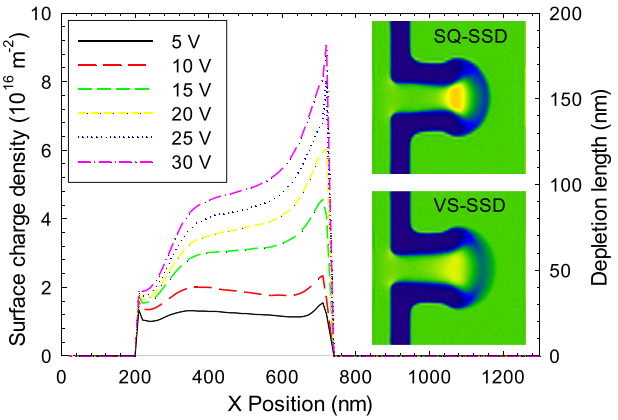

FIG. 3. Surface charge along the sidewalls of the trenches defining the channel for different bias in the SQ-SSD for a width of 300 nm. The insets show the 2D chart of average electron concentration at 30 V in the SQ-SSD with $W = 300$ nm and the VS-SSD with $W_i = 300$ nm and $W_o = 400$ nm.

of this effect.[18] In fact, based on the thermal study made on SQ-SSDs,[19] we estimate that VS-SSDs can generate Gunn oscillations at temperatures below 450 K, thus avoiding the strong drop of efficiency that occurs when the devices operate above that temperature.

The origin of the absence of Gunn oscillations in the SQ-SSD with $W = 300$ nm can be identified, thanks to the values of the surface charge density along the semiconductor-air interface in the channel plotted in Fig. 3. The high value of the surface charge at the exit of the channel, which increases with the voltage (note that a self-consistent model for the surface effects is used, thus σ depends on the bias and position[12,14]), inhibits the nucleation of charge domains. It can be observed that when the bias is higher than 15 V, the theoretical depletion width at each side of the channel (estimated as $W_d = \sigma/N_{Db}$) exceeds 100 nm at the exit, thus significantly reducing its effective width. This effect is illustrated in the insets of Fig. 3, where 2D charts of the average electron concentration at 30 V in the SQ-SSD ($W = 300$ nm) and in the VS-SSD ($W_i = 300$ nm $W_o = 400$ nm) are shown. The depletion at the anode side of the channel of the SQ-SSD, preceded by a strong accumulation of carriers, is clearly visible, while in the VS-SSD this effect is smoothed thanks to its opening at the exit.

Even if static/average magnitudes can provide significant information, a detailed study of the time evolution of the electron concentration and electric field is compulsory for the correct understanding of the dynamics of the Gunn oscillations in GaN SSDs. Fig. 4(a) shows current sequences at 30 V for a SQ-SSD with $W = 500$ nm, and a VS-SSD with $W_i = 300$ nm $W_o = 400$ nm, both presenting Gunn oscillations with similar frequency, around 400 GHz. Figs. 4(b) and 4(c) show the profiles of U-valley occupation and electric-field for the SQ- and VS-SSDs, respectively, at four successive time moments evenly spaced within a period of the oscillation (indicated in Fig. 4(a) with colored circles). At first sight, the two sets of profiles show the typical behavior of Gunn domains, which is the motion of a high field/accumulation region given by the electrons transferred to the upper valleys. However, with a more detailed inspection some differences can be observed. In the SQ-SSD, one can see that

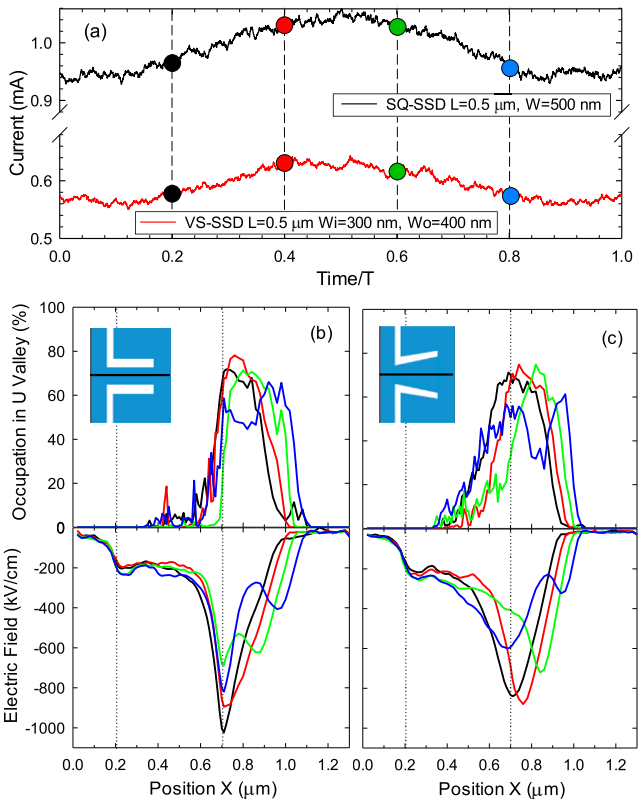

FIG. 4. (a) One period current sequence for the SQ-SSD with $W = 500$ nm and the VS-SSD with $W_i = 300$ and $W_o = 400$ nm at 30 V. The colored circles mark the equidistant time moments in which the instantaneous profiles of U-valley occupation and electric field along the centre of the channel reported in (b) and (c), for the SQ-SSD and VS-SSD, respectively, were calculated. The position of the channel is indicated by the vertical dotted lines.

the formation of the high field region takes place just at the exit of the channel, reason why a long enough distance $L_a = 600$ nm is required to let the domain being fully thermalized and not interfere with the Gunn process. This happens due to the increase of the surface charges at that position, see Fig. 3, that strongly enhance the electric field (taking at that point its maximum value). In the case of the VS-SSD, the domain is created well inside the channel, at around its middle point. This happens because the distribution of the electric field in the channel is more homogeneous than in the SQ-SSD due to the leaned trenches and the less pronounced increase of surface charges at the anode side. As a consequence, in the VS-SSD the point at which the threshold field for negative differential mobility in GaN ($E_{th} = 250$ kV/cm) is reached is shifted towards the inner part of the channel. Under these conditions, the modulation of the electric field related to the transit of the high-field domain is improved, so that Gunn oscillations are obtained for lower applied voltages in the VS-SSDs (in spite of the higher maximum field provided by the SQ-SSD).

Fig. 5 shows the frequency and amplitude of the oscillations found in the VS-SSDs as a function of the bias. The values of f_{Gunn} are in the range 300–500 GHz (similar to those obtained for SQ-SSDs in previous works[12]), with decreasing values as the voltage increases from 20 V up to 50 V. One can notice that the reported frequencies are similar for both W_i, and slightly lower when W_o is widened (since the Gunn domain is formed at a longer distance from the exit

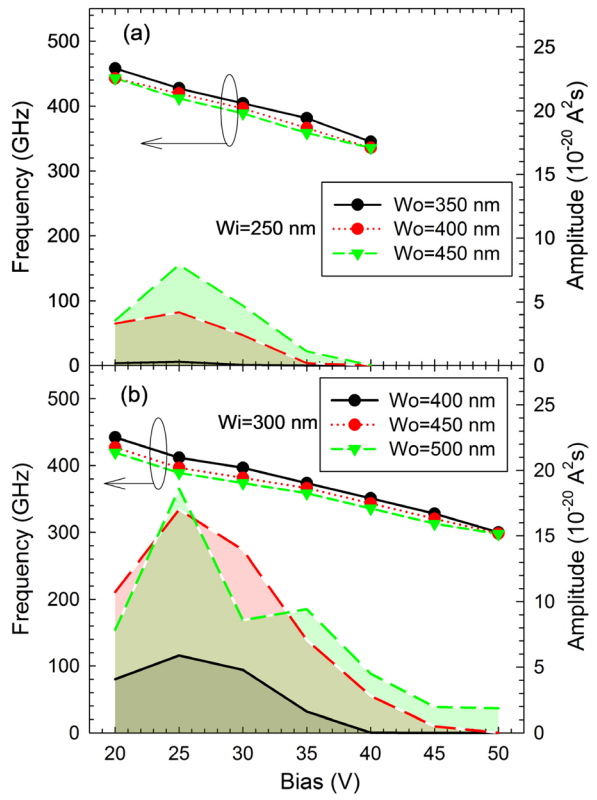

FIG. 5. Frequency and amplitude of the oscillations vs. applied voltage for 500 nm long VS-SSDs with different W_o and (a) $W_i = 250$ nm and (b) $W_i = 300$ nm.

of the channel). Concerning the amplitude of the oscillations, the maximum is found at 25 V for all the geometries, and, as expected due to the higher level of DC current (plotted in Fig. 1), higher values are obtained for larger W_i. Regarding the value of W_o, an increase of its value is able to improve the amplitude of the oscillations, but only up to a certain limit. A further widening of the exit decreases the efficiency, since the amplitude saturates while the DC current grows. For example, for $W_i = 300$ nm, the optimum value found for W_o is 450 nm.

In conclusion, the regular geometry of the SQ-SSD has some limits for the generation of Gunn oscillations, mainly in GaN, since the high applied voltages strongly modify the distribution of the surface charges, leading to the narrowing of the effective width at the exit of the channel. The V-shape geometry proposed here allows decreasing the threshold voltage needed for the onset of Gunn oscillations, which are achieved with much lower DC current, thus improving the DC to AC efficiency and reducing the thermal dissipation issues (which are of key importance from a practical point of view).

This work was partially supported by the European Commission through the ROOTHz Project ITC-2009-243845, by the Dirección General de Investigación (MICINN) through the Project TEC2010-15413, and by the Consejería de Educación de la Junta de Castilla y León through the Projects SA183A121 and SA052U13.

[1]C. Mann, in *Proceedings of the IEEE/MTT-S International Microwave Symposium* (IEEE, 2007), p. 1705.
[2]T. H. Crowe, W. L. Bishop, D. W. Porterfield, J. L. Hesler, and R. M. Weikle, IEEE J. Solid-State Circuits **40**, 2104 (2005).
[3]A. M. Song, M. Missous, P. Omling, A. R. Peaker, L. Samuelson, and W. Seifert, Appl. Phys. Lett. **83**, 1881 (2003).
[4]C. Balocco, S. R. Kasjoo, X. F. Lu, L. Q. Zhang, Y. Alimi, S. Winnerl, and A. M. Song, Appl. Phys. Lett. **98**, 223501 (2011).
[5]C. Balocco, M. Halsall, N. Q. Vinh, and A. M. Song, J. Phys.: Condens. Matter **20**, 384203 (2008).
[6]A. Westlund, P. Sangaré, G. Ducournau, P.-Å. Nilsson, C. Gaquière, L. Desplanque, X. Wallart, and J. Grahn, Appl. Phys. Lett. **103**, 133504 (2013).
[7]P. Sangaré, G. Ducournau, B. Grimbert, V. Brandli, M. Faucher, C. Gaquière, A. Iñiguez-de-la-Torre, I. Iñiguez-de-la-Torre, J.-F. Millithaler, J. Mateos, and T. González, J. Appl. Phys. **113**, 034305 (2013).
[8]E. Alekseev and D. Pavlidis, Solid-State Electron. **44**, 941–947 (2000).
[9]K. Y. Xu, G. Wang, and A. M. Song, Appl. Phys. Lett. **93**, 233506 (2008).
[10]J. Mateos, B. G. Vasallo, D. Pardo, and T. González, Appl. Phys. Lett. **86**, 212103 (2005).
[11]I. Iñiguez-de-la-Torre, J. Mateos, D. Pardo, A. M. Song, and T. González, Int. J. Numer. Modell.: Electron. Networks, Devices Fields **23**, 301–314 (2010).
[12]A. Iñiguez-de-la-Torre, I. Iñiguez-de-la-Torre, J. Mateos, T. González, P. Sangaré, M. Faucher, B. Grimbert, V. Brandli, G. Ducournau, and C. Gaquière, J. Appl. Phys. **111**, 113705 (2012).
[13]C. Jacoboni and P. Lugli, *The Monte Carlo Method for Semiconductor, Device Simulation* (Springer, Vienna, 1989).
[14]I. Iñiguez-de-la-Torre, J. Mateos, T. González, D. Pardo, J. S. Galloo, S. Bollaert, Y. Roelens, and A. Cappy, Semicond. Sci. Technol. **22**, 663 (2007).
[15]J. Mateos, T. González, D. Pardo, V. Hoel, H. Happy, and A. Cappy, IEEE Trans. Electron. Devices **47**, 250 (2000).
[16]S. García, S. Pérez, I. Íñiguez-de-la-Torre, J. Mateos, and T. González, J. Appl. Phys. **115**, 044510 (2014).
[17]J. B. Gunn, Solid State Commun. **1**, 88 (1963).
[18]O. Yilmazoglu, K. Mutamba, D. Pavlidis, and T. Karaduman, IEEE Trans. Electron Devices **55**, 1563 (2008).
[19]J.-F. Millithaler, I. Iñiguez-de-la-Torre, T. González, P. Sangaré, G. Ducournau, C. Gaquière, and J. Mateos, in *Spanish Conference on Electron Devices* (IEEE, 2013), pp. 45–48.